POLITECNICO DI TORINO
Repository ISTITUZIONALE

Achieving 99.75% water recovery in industrial groundwater remediation: contaminant removal and feasibility of a multibarrier treatment train targeting near-zero liquid discharge

Original
Achieving 99.75% water recovery in industrial groundwater remediation: contaminant removal and feasibility of a multibarrier treatment train targeting near-zero liquid discharge / Craveri, L., Bertozzi, E., Malaguti, M., Copetti, G., Cerrina, D., Trombetta, A., Rosetti, V., Tiraferri, A.. - In: NPJ CLEAN WATER. - ISSN 2059-7037. - 9:74(2026). [10.1038/s41545-026-00579-2]

Availability:
This version is available at: 11583/3016329 since: 2026-10-05T12:26:40Z

Publisher:
Springer

Published
DOI:10.1038/s41545-026-00579-2

Terms of use:

This article is made available under terms and conditions as specified in the corresponding bibliographic description in the repository

Publisher copyright

(Article begins on next page)

14 November 2026

npj | clean water

Article

Published in partnership with King Fahd University of Petroleum & Minerals

https://doi.org/10.1038/s41545-026-00579-2

Achieving 99.75% water recovery in industrial groundwater remediation: contaminant removal and feasibility of a multibarrier treatment train targeting near-zero liquid discharge

Check for updates

Lorenzo Craveri[1,5], Erica Bertozzi[1,5], Marco Malaguti[1], Gabriele Copetti[1], Davide Cerrina[1,2], Alessandro Trombetta[3], Valentina Rosetti[3] & Alberto Tiraferri[1,4] ✉

This study evaluates advanced water treatment technologies to remediate industrially contaminated groundwater under a 99.75% water recovery target for near-zero liquid discharge. Laboratory batch tests on real groundwater assessed pre-oxidation–coagulation–flocculation, activated carbon andferric hydroxide adsorption, reverse osmosis, and chemical treatments. The synergy of the selected techniques was investigated for the first time to remove specific amine-containing compounds and sulfolane. Removal rates exceeded 95% for most metals and several organics, whereas aliphaticaldehydes were found to be recalcitrant. The selected techniques were then incorporated into a multi-barrier treatment train, tested with 300 L of real groundwater under the 99.75% water recovery target. Sulfolane concentration decreased by 99.6%, amines concentrations were reduced below detection, naphthalene removal exceeded 99%, and most heavy metals were removed by >95%. Aliphaticaldehydes increased during pre-treatment and required targeted post-membrane chemical treatment to meet regulatory, while vanadium showed variable behavior. The results demonstrate that integrated treatment enables regulatory compliance and minimal liquid discharge, although persistent compounds require specific multi-barrier strategies.

Groundwater is a critical resource for drinking water, agriculture, and industry[1,2], supplying nearly half of the world's population with drinking water and accounting for about 40% of irrigation needs[3,4]. However, its quality is increasingly threatened by industrial activities, chemical spills, and legacy waste disposal, with both regulated and emerging contaminants compromising aquifer systems and posing risks to human health[1,5,6]. While remediation of contaminated aquifers is enforced under both European Union and Italian national legislation (Directive 2000/60/EC and D.Lgs. 152/2006), restoring these resources to safe and sustainable use remains challenging, particularly as regulatory requirements for effluent quality and discharge become increasingly stringent[7–9]. Treatment strategies for industrially impacted groundwater and remediation of polluted sites are typically site-specific and tailored to the local conditions and contaminant profiles. Despite this flexibility in design, such approaches often fail to meet regulatory thresholds, especially when dealing with complex mixtures, recalcitrant compounds, and persistent transformation by-products[10,11]. In situ remediation technologies, such as the injection of reactive or sorptive materials, e.g., nanoscale zero-valent iron, activated carbon, or electron donor compounds, and permeable reactive barriers, have demonstrated potential, but remain limited in full-scale applications[12–14]. As a result, pump-and-treat systems coupled with ex situ treatment continue to be the most commonly implemented technology[10,15–17]. Yet, the increasing complexity of groundwater contamination underscores the inadequacy of single-unit processes, especially when targeting a wide range of contaminants.

[1]Department of Environment, Land and Infrastructure Engineering, Politecnico di Torino, Torino, Italy. [2]Dipartimento di Chimica, Università di Torino, Torino, Italy. [3]Eni Rewind S.p.A., Milan, Italy. [4]Clean Water Center (CWC), Politecnico di Torino, Turin, Italy. [5]These authors contributed equally: Lorenzo Craveri, Erica Bertozzi. ✉e-mail: alberto.tiraferri@polito.it

The limitation of single-unit processes when dealing with complex matrices has led to the progressive adoption of multibarrier treatment trains, which combine complementary physical, chemical, and biological processes for robust contaminant removal[9]. Typical configurations integrate technologies such as coagulation–flocculation, membrane filtration, adsorption, advanced oxidation, and biological polishing to address the broad spectrum of compounds found in contaminated groundwater[18–21]. High water recovery rates and, ideally, zero liquid discharge (ZLD) are increasingly prioritized to minimize waste streams and maximize the reuse of treated water. Although ZLD or minimal liquid discharge strategies generally require higher energy input and capital costs, they can reduce environmental discharges, limit secondary waste generation, and enhance long-term sustainability, potentially offsetting initial investments[22–24]. The need for robust multibarrier solutions is further driven by the evolving nature of groundwater contamination. Industrial activities often introduce complex and poorly characterized contaminant mixtures into groundwater, including compounds such as sulfolane, alkanolamines, and halogenated by-products[25–27]. Despite growing regulatory attention, literature on the efficacy of treatment processes for removing these compounds, especially in systems engineered for near-ZLD, remains scarce[28,29]. The lack of detailed studies on removal efficiencies, by-product formation, and operational bottlenecks for these and similar contaminants presents a major barrier to the design of robust and sustainable remediation solutions. Addressing these challenges requires a deeper understanding of process performance under realistic conditions, in real matrices, and at high water-recovery rates.

Motivated by these considerations, the present study aims to bridge this knowledge gap through a comprehensive experimental investigation of a sequential, multibarrier treatment train for the remediation of real-matrix groundwater sourced from a contaminated industrial site. First, the performance of individual unit operations, namely, pre-oxidation, coagulation–flocculation-sedimentation, ultrafiltration, adsorption on granular activated carbon and ferric oxide-hydroxide, reverse osmosis, and chemical treatments, is evaluated against a diverse suite of contaminants. Building on these results, the most effective steps are integrated into a complete treatment train designed to operate at a target water recovery of 99.75%. The study provides a comprehensive dataset on contaminant removal and transformation under near-zero liquid discharge conditions, with particular focus on sulfolane, alkanolamines, and aliphatic aldehydes in real groundwater. The novelty of this work lies in the integration of established unit operations into a previously unreported high-recovery treatment configuration, combined with a system-level investigation of contaminant behavior and transformation pathways under minimal liquid discharge conditions.

Results and discussion

Transformation of contaminants by pre-oxidation–coagulation–flocculation (OCF)

The OCF process was evaluated as a pre-treatment step to promote the chemical transformation and partial removal of a broad range of contaminants, primarily heavy metals and suspended solids, and to a lesser extent, organic compounds.

Figure 1 presents the transformation percentage of these compounds in OCF, including pre-oxidation with either sodium hypochlorite (NaOCl) at pH 10 or chlorine dioxide (ClO_2) at pH 8.5. Both oxidants were followed by identical coagulation–flocculation sequences, with contaminant transformation assessed across three replicate experiments. Positive values indicate net degradation or removal, while negative values reflect the formation of compounds during treatment.

The removal of heavy metals, the primary target of the process, showed strong but variable performance, depending on both the metal and the oxidant. Iron, manganese, and zinc were almost entirely removed by both oxidants (removal rates of 99–100%), proving the robustness of the process for these elements. Notably, ClO_2 achieved complete removal of aluminum and vanadium (100%), whereas NaOCl only partially removed these metals

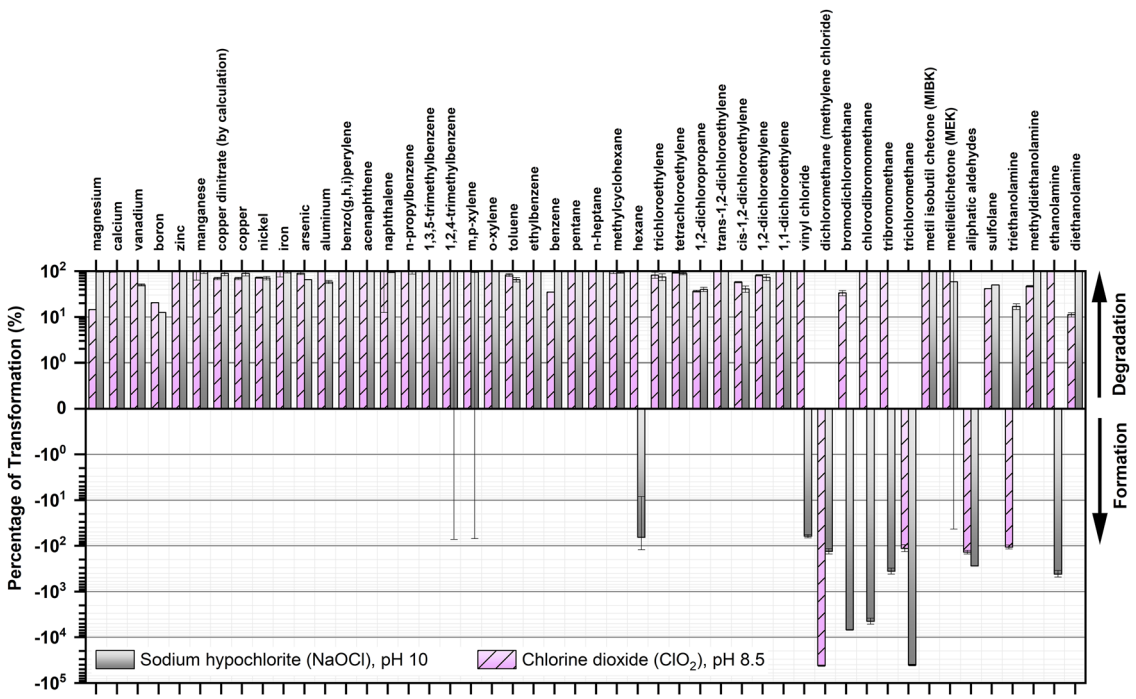

Fig. 1 | Percentage transformation of contaminants in the physico-chemical pre-treatment unit consisting of an oxidation–coagulation–flocculation process (OCF). Transformation was calculated as $\left(1-\frac{c_{FIN}}{c_0}\right)\times 100$, where c_0 is the influent concentration, and c_{FIN} is the effluent concentration. Bars represent the mean ± one standard deviation from three independent replicate experiments. Gray solid bars correspond to treatment with sodium hypochlorite at pH 10, while pink patterned bars represent treatment with chlorine dioxide at pH 8.5. Negative values indicate formation of the compound during the process, while positive values indicate degradation. Note that the y-axis shows the magnitude of transformation on a symmetric logarithmic (symlog) scale: values between +1 and −1 are shown on a linear scale, while larger positive and negative values are displayed logarithmically.

(58% for aluminum and 50% for vanadium). This suggests greater oxidative effectiveness of ClO_2 for certain oxyanions and amphoteric metals. For arsenic, nickel, and copper, both oxidants achieved moderate removal rates, ranging between 65% and 90%, with only minor differences between the two oxidants. Overall, these results confirm that OCF can be highly effective for a subset of heavy metals, although optimization of oxidant type and dose is required to maximize removal across all relevant species.

The abatement of organic contaminants also depended on both chemical structure and oxidant choice. Alkanolamines, such as DEA and MDEA, were completely degraded by NaOCl (100%), whereas ClO_2 achieved only partial removal (11–47%). In contrast, MEA was efficiently removed by ClO_2 (100%) but formed in large quantities with NaOCl (−415%). Beyond highlighting divergent oxidation pathways between the two oxidants, this trend suggests that NaOCl under alkaline conditions promoted the partial oxidative fragmentation of nitrogenous precursors, consistent with the release of smaller, more mobile amine species, such as MEA, from higher molecular weight alkanolamines[30]. Triethanolamine followed an opposite trend, with partial removal via NaOCl (17%) and substantial formation under ClO_2 treatment (−107%).

For carbonyl and halogenated organics, additional divergent trends were observed. Both MEK and MIBK were efficiently degraded by both oxidants (MEK: 59% with NaOCl, 100% with ClO_2; MIBK: 100% with both), highlighting the strong reactivity of these oxidants toward certain ketones. In contrast, aliphatic aldehydes were generated during both treatments (−275% with NaOCl, −138% with ClO_2), likely reflecting oxidative cleavage of precursor compounds. This accumulation can be attributed to incomplete mineralization of recalcitrant organic carbon species, where low molecular weight carbonyl compounds, such as acetaldehyde and MEK, represent common and stable oxygenated intermediates[31–33].

Importantly, the formation of halomethanes and other halogenated species, consistent with hypochlorite-driven electrophilic substitution reactions, was observed for both oxidants, albeit with different by-product profiles[32,34]. While NaOCl promoted the massive formation of trichloromethane (−40,000%) and a substantial overall increase in halomethanes and vinyl chloride, ClO_2 only produced trichloromethane and dichloromethane (−41,000% for ClO_2 vs. −133% for NaOCl). The more pronounced formation of trichloromethane and halogenated by-products observed in the presence of NaOCl is consistent with previous studies[35,36]. Despite by-product formation, the two oxidants were chosen as they are cost-effective and readily scalable in full-scale plants, rather than laboratory-optimized solutions. Although advanced oxidation processes (e.g., ozonation, UV-based systems, Fenton) could reduce certain by-products, they do not eliminate the need for downstream polishing steps and entail higher operational complexity, costs, and safety requirements compared to ClO_2 and NaOCl[37–39]. To clarify the overall picture of compound formation, transformation values should be interpreted in conjunction with absolute influent and effluent concentrations (see Table S3 of the SI). In fact, the compounds exhibiting high formation percentages in OCF were mostly associated with very low influent concentrations (below 0.6 µg/L), with the exception of ethanolamine and triethanolamine, which showed inlet values of 1.12 µg/L and 3 µg/L, respectively, and aliphatic aldehydes that recorded inlet values of 95.8 µg/L. Overall, ClO_2 produced far fewer regulated disinfection by-products, confirming to be a strong yet more selective oxidant with a lower halogenating potential compared to NaOCl[40–42]. These findings underscore the trade-offs between the two oxidants, as ClO_2 systems are more complex and expensive to install and operate than NaOCl, due to the need for on-site generation and additional safety controls[43–45]. Although a comprehensive by-product identification was not performed and a detailed mechanistic interpretation was beyond the scope of this study, the systematic quantification of negative removals, i.e., compound formation during pre-oxidation, provides insight into transformation pathways that are rarely documented for industrial groundwater matrices and are critical for rational multibarrier design.

Adsorption of selected contaminants on granular activated carbon

The adsorption of selected contaminants onto vegetal GAC was systematically investigated to assess the effectiveness of this treatment step for removing key organic pollutants from water. Figure 2 presents adsorption isotherms for several priority compounds, including sulfolane, MEA, DEA, MDEA, TEA, and the class of aliphatic aldehydes, along with corresponding Freundlich model fits. Panels (a–f) of Fig. 2 show the relationship between equilibrium aqueous concentration and the amount adsorbed per gram of GAC. The adsorption isotherms reported here constitute one of the first quantitative datasets for these compounds on GAC under realistic groundwater conditions. Multiple independent experiments confirm the reproducibility of the observed trends for each compound. The Freundlich model provided a very good fit for the data, with K and n parameters (and the linearized isotherm equations with the R^2 coefficients) reported in each panel. The parameter n ranged from 1.09 for aliphatic aldehydes to 2.62 for DEA, indicating substantial differences in adsorption intensity. A clear hierarchy in adsorbability emerged: MDEA and sulfolane exhibited the highest adsorption capacities, followed by DEA, then TEA, MEA, and finally the aliphatic aldehydes. Medium to high adsorption capacity for acetaldehydes was also observed (*data not shown*). These differences reflect the influence of molecular size, polarity, and functional group chemistry, with larger and more hydrophobic amines showing stronger interactions with GAC. Panels (g) and (h) in Fig. 2 present modeled adsorption isotherms for all compounds across wide (g) and narrow (h) ranges of equilibrium concentrations, based on the fitted Freundlich parameters. These panels and the related equations are valuable for practical applications, as they enable estimation of GAC consumption rates for any given influent contaminant concentration beyond this work.

Effluent monitoring of GAC adsorption columns, as illustrated in Fig. S2 and discussed in detail in Supplementary Results S1 (SI), was highly consistent with batch experiments and further substantiates the observed equilibrium adsorption trends. Together, batch and column results confirm that GAC adsorption, when appropriately designed and managed, provides reliable removal of a spectrum of organic contaminants in continuous-flow systems, but it may not be sufficient to guarantee the effective removal of the more hydrophilic amines or aliphatic aldehydes.

Evaluation of reverse osmosis membranes

The technical performance of three commercial RO membranes, XLE, BW30, and SW30, was assessed in laboratory-scale batch experiments, focusing on both water flux and the rejection of selected organic micropollutants. Key results are summarized in Fig. 3, while Fig. S3 (SI) presents the same data in an alternative format to facilitate comparison across membranes. Panels (a–c) of Fig. 3 show the expected trend of declining water flux with increasing recovery for all membranes. The XLE membrane delivered the highest initial flux at moderate pressure, followed by BW30 and then SW30, which operated at the highest pressure and exhibited the lowest but most stable flux across the recovery range.

The system rejection results (Fig. 3, panels d–i) reveal pronounced differences in contaminant removal among the three membranes. The SW30 membrane achieved the highest and most consistent rejection rates, generally reaching or exceeding 99% for most compounds, including sulfolane and MDEA. This high performance is attributed to its tight, compact pore structure, making it especially suited for applications where compliance with strict regulatory limits is necessary[46]. The BW30 membrane exhibited high rejection for larger or more hydrophobic compounds, such as DEA, MDEA, and TEA, but showed reduced performance for more hydrophilic, lower molecular weight contaminants like sulfolane and MEA. The BW30 membrane also exhibited near complete rejection of glycols and MEK (*data not shown*). On the other hand, the XLE membrane, while offering the highest permeability, displayed notably lower rejection efficiencies, particularly for sulfolane, MEA, and aliphatic aldehydes. A key finding is the particularly low rejection rates observed for aliphatic aldehydes, with only about 60% removal by SW30 and approximately 30% by

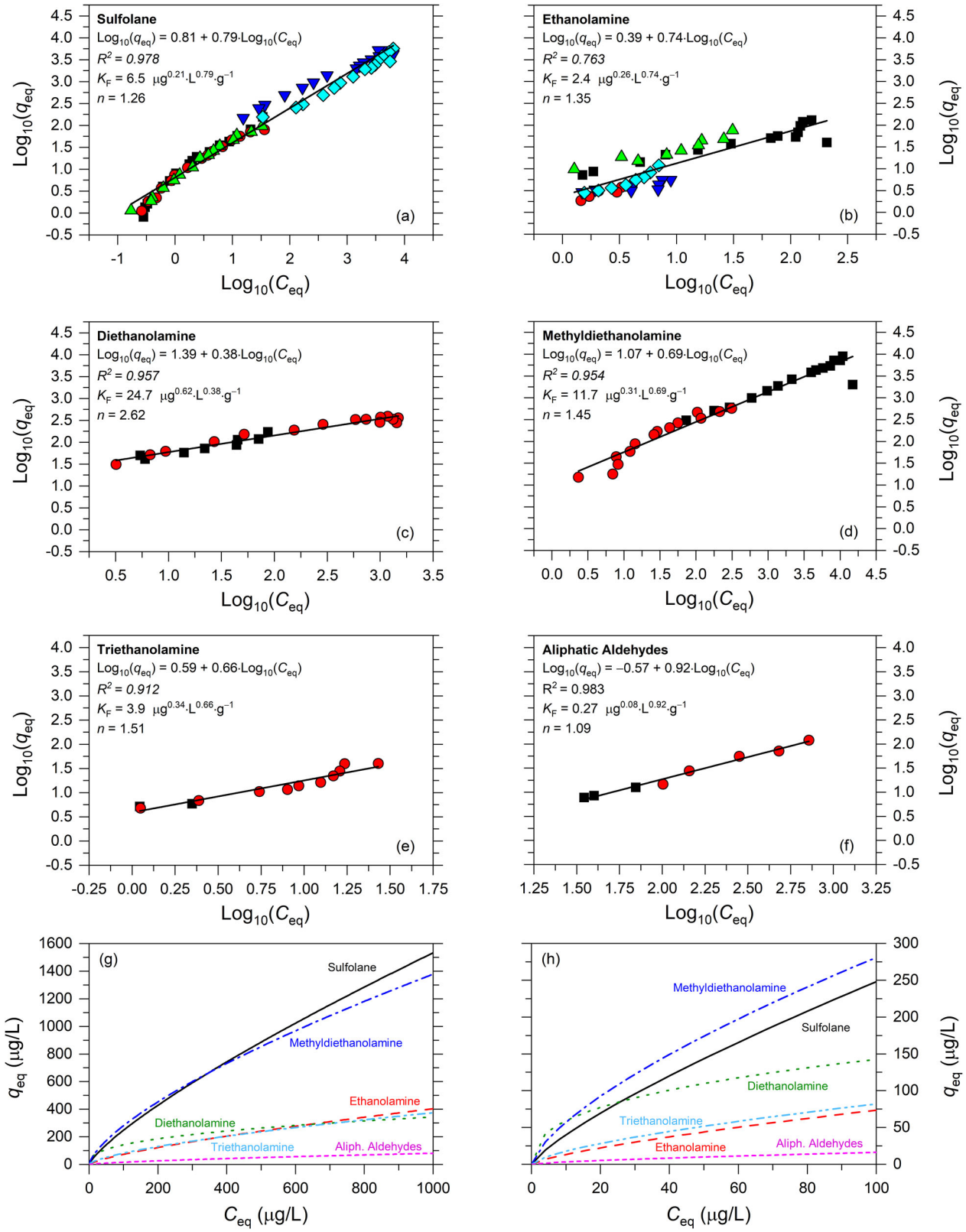

Fig. 2 | Adsorption isotherms of selected compounds on vegetal granular activated carbon (GAC). a–f show experimental data (symbols) and corresponding Freundlich model fits (black lines), expressed as $q_{eq} = K_F C_{eq}^{\frac{1}{n}}$, and linearized as $Log_{10} q_{eq} = Log_{10} K_F + \frac{1}{n} Log_{10} C_{eq}$. Different symbols represent independent experiments. The estimated Freundlich parameters, K_F and n, along with the linearized equations, are reported in each panel. **g–h** present the modeled adsorption isotherms for all compounds based on the parameters evaluated by the Freundlich model, over a wide (**g**) and a narrow (**h**) range of equilibrium concentrations, C_{eq}, based on the fitted parameters.

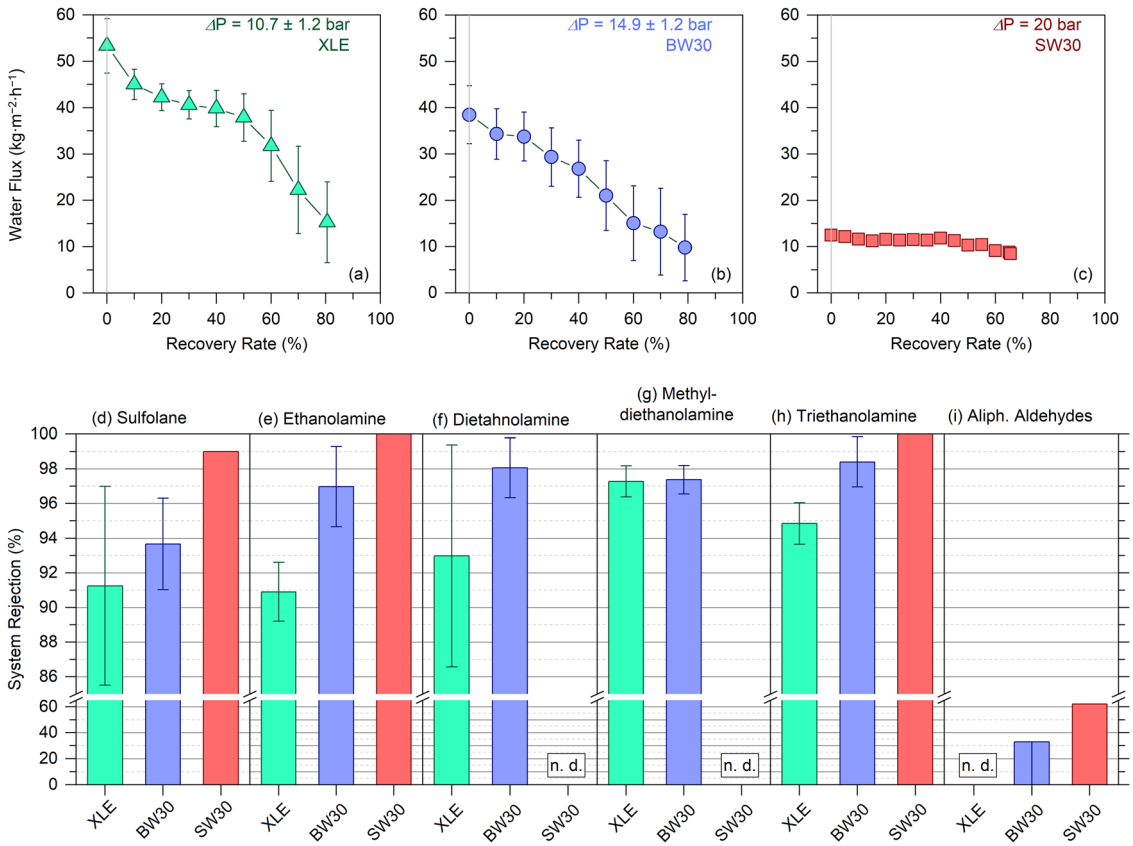

Fig. 3 | Performance of different reverse osmosis membranes in terms of water flux and compound rejection based on lab-scale batch experiments. a–c show measured water flux (LMH) as a function of recovery rate for the XLE (**a**; green triangles), BW30 (**b**; blue circles), and SW30 (**c**; red squares) membranes. The applied hydraulic pressure for each membrane is indicated in the respective panel. Data points represent the mean ± one standard deviation from six (XLE) or seven (BW30) independent replicate experiments; no replicates were performed for SW30. Lines connecting the data points are included solely as a visual aid. **d–i** present system rejection values for six selected compounds (indicated above each plot). System rejection was calculated as $\left(1-\frac{c_{P,TOT}}{c_{F,0}}\right)\times 100$, where $c_{F,0}$ is the initial feed concentration and $c_{P,TOT}$ is the concentration in the total permeate volume collected. Bars represent the average rejection observed for the XLE (leftmost; green), BW30 (middle; blue), and SW30 (rightmost; red) membranes. A y-axis break is inserted from approximately 60% to 85% to improve graph readability. "n.d." indicates that no data were determined for that specific case.

BW30. Small, highly polar molecules, such as simple aldehydes, can permeate polyamide RO membranes due to their small molecular size and weak interactions with the membrane matrix[38,47].

These results underscore that, given the need to achieve extremely high overall water recovery values (approaching 99.75% in this treatment system), the rejection rates for individual contaminants must also be extremely high to ensure a high-quality permeate. Evaluating membrane rejection under such high-recovery constraints is essential, as concentration polarization and solute buildup substantially alter apparent performance compared to conventional low-recovery laboratory tests typically reported in the literature. This is especially important for contaminants such as sulfolane and methyldiethanolamine, which require high removal rate to meet treatment objectives (see Table 1), as well as for compounds like aliphatic aldehydes and ethanolamine, which may be formed during OCF (see Fig. 1) and are more challenging to reject. This finding implies the need for the selection of high-rejection membranes to achieve reliable removal of all critical contaminants in the application investigated in this work.

Removal of aliphatic aldehydes and implications for boron introduction

Aliphatic aldehydes have emerged as a particularly challenging class of contaminants in the unit operations discussed above. As established in previous sections, these compounds formed during OCF, likely due to oxidative cleavage of precursor organics[36]. Removal via GAC adsorption and RO membranes was found to be limited, with rapid breakthrough in GAC columns and low RO rejection rates, even for the most selective SW30 membrane. To address this critical gap, additional targeted treatment processes were explored, as illustrated in Fig. 4. Batch chemical reduction tests using sodium borohydride ($NaBH_4$) demonstrated that aliphatic aldehydes can be efficiently removed through reductive transformation. As shown in panel (a), $NaBH_4$ achieved suitable removal, achieving up to 95% reduction in aldehyde concentration at the highest tested dose. $NaBH_4$ reduction proceeds via nucleophilic hydride transfer to the carbonyl group, converting aldehydes into the corresponding alcohols[48]. Note that no significant transformation of acetaldehyde was observed through the use of NaOCl. However, the use of $NaBH_4$ results in the introduction of boron as a secondary contaminant, which is regulated by a discharge limit of 1 mg/L in the final effluent. Alternative strategies, such as biological polishing processes and advanced oxidation processes, were evaluated but not pursued due to matrix-related constraints, including toxicity and limited compatibility, and higher operational complexity and associated costs[39,49,50]. Panel (b) of Fig. 4 tracks the concentration of aliphatic aldehydes across a preliminary test comprising sequential treatment steps. Following OCF, RO (BW30), and chemical reduction, there was a substantial decrease in aldehyde concentration. Further GAC and GFH filtration brought levels close to or below the regulatory threshold (indicated by the red dashed line), confirming that a multi-barrier approach, including a chemical degradation step, can effectively manage even highly persistent compounds when properly designed.

To quantitatively address the boron introduction, a mass balance was performed linking $NaBH_4$ dosage to the resulting boron

Table 1 | Influent (average and peak) concentrations, effluent limit concentrations, and resulting required removal rate (%) for the compounds exceeding regulatory limits

	Expected average influent concentration	Expected peak influent concentration	Effluent limits	Required removal rate considering average concentrations	Minimum (DESIGN) removal rate based on peak influent concentration
	µg/L	µg/L	µg/L	%	%
Amines					
Diethanolamine (DEA)	1.3	5.4	4.2	0	22.22
Methyldiethanolamine (MDEA)	7	446.6	3.9	44.29	99.13
Triethanolamine (TEA)	2	6.6	3.9	0	40.91
Sulfur-containing compounds					
Sulfolane	307.3	1909.9	0.138	99.955	99.993
Aldehydes and ketones					
Acetaldehyde	0.7	5.8	1.47	0	74.66
Organohalogen compounds					
Trichloromethane (chloroform)	0.2	0.4	0.15	25.00	62.50
Tetrachloroethylene	1.3	4.3	1.1	15.38	74.42
Alkanes					
Methylcyclohexane	3.5	32.3	0.12	96.57	99.63
Pentane	0.1	0.4	0.12	0	70
Total hydrocarbons as hexane	177.1	1930.8	350	0	81.87
Aromatic hydrocarbons (BTEX and Alkylbenzenes)					
Benzene	0.2	3.2	1	0	68.75
o-xylene	0.3	0.7	0.198	34.00	71.71
1,2,4-trimethylbenzene	1.1	21.6	0.138	87.45	99.36
1,3,5-trimethylbenzene	0.1	1.6	0.126	0	92.13
n-propylbenzene	3.1	14.2	0.114	96.32	99.20
Polycyclic aromatic hydrocarbons (PAHs)					
Naphthalene	0.4	2.4	0.0054	98.65	99.78
Acenaphthene	0.03	0.09	0.0081	73.00	91.00
Inorganic elements and ions					
Iron	2348.6	6064.8	200	91.48	96.70
Nickel	8.6	82.2	20	0	75.67
Copper dinitrate (by calculation)	6.1	49.3	7.8	0	84.18
Manganese	2722.9	5596.1	50	98.16	99.11
Full list of monitored parameters					

Amines: diethanolamine (DEA), ethanolamine (MEA), methyldiethanolamine (MDEA), triethanolamine (TEA), filming amines, piperazine. **Sulfur-containing compounds:** sulfolane. **Aldehydes and Ketones:** aliphatic aldehydes, acetaldehyde, methyl ethyl ketone (MEK), methyl isobutyl ketone (MIBK). **Organohalogen Compounds:** trichloromethane (chloroform), tribromomethane, chlorodibromomethane, bromodichloromethane, dichloromethane (methylene chloride), vinyl chloride, 1,1-dichloroethylene, 1,2-dichloropropane, 1,2-dichloroethylene, tetrachloroethylene, trichloroethylene, sum of organohalogen compounds. **Alkanes:** hexane, methylcyclohexane, n-heptane, pentane, total hydrocarbons as hexane, hydrocarbons C<10. **Aromatic Hydrocarbons (BTEX and Alkylbenzenes):** benzene, ethylbenzene, toluene, o-xylene, m,p-xylene, 1,2,4-trimethylbenzene, 1,3,5-trimethylbenzene, n-propylbenzene. **Polycyclic Aromatic Hydrocarbons (PAHs):** naphthalene, acenaphthene, dibenzo(a.e)pyrene, dibenzo(a.i)pyrene, dibenzo(a.l)pyrene, dibenzo(a.h)pyrene, benzo(g,h,i)perylene, sum of PAHs (polycyclic aromatic hydrocarbons). **Glycols:** ethylene glycol, diethylene glycol, triethylene glycol. **Inorganic Elements and Ions:** aluminum, arsenic, iron, lead, nickel, copper, copper dinitrate (by calculation), manganese, vanadium, zinc, boron, chlorides, free active chlorine. **Environmental and Other Parameters:** total suspended solids, total dissolved solids, pH, and chemical oxygen demand.

The full list of the compounds monitored in this study is reported in the last row of the table, while the complete list with the respective values is reported in Fig. S1.

concentration, showing good agreement between theoretical (0.572 and 1.43 mg/L for 2 and 5 mg/L $NaBH_4$, respectively) and measured values (0.562 and 1.30 mg/L, Fig. 4d). Panels (c) and (d) of Fig. 4 examine boron behavior during treatment. Panel (c) highlights the limited adsorption of boron on GAC[51,52], while GFH shows somewhat greater affinity and removal capacity. Panel (d) demonstrates that, following chemical reduction with $NaBH_4$, subsequent filtration with GFH effectively reduced boron concentrations to below the regulatory limit in all tests where it was applied.

For completeness, the ability of GFH to retain aliphatic aldehydes was also tested: as shown in Fig. S4 (SI), GFH exhibited minimal adsorption capacity for these compounds across the tested concentration range, indicating that it would not provide a substantial barrier for aldehyde removal.

Management of vanadium in the treatment train

Vanadium is a trace element of regulatory concern due to its stringent discharge limits. In preliminary tests, the OCF step typically resulted in significant vanadium removal, particularly when chlorine dioxide was used

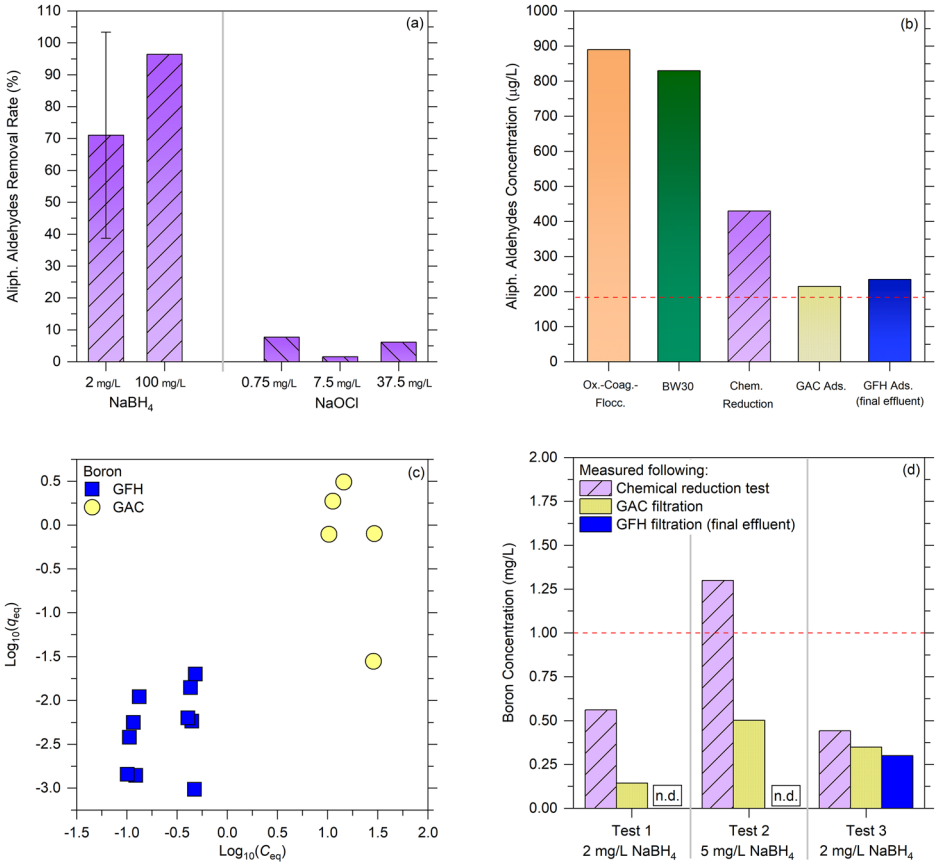

Fig. 4 | Behavior of aliphatic aldehydes and boron during selected treatment steps. a Percentage removal of aliphatic aldehydes in batch chemical reduction tests using two different concentrations of sodium borohydride ($NaBH_4$). For the 2 mg/L $NaBH_4$ test (corresponding to 0.57 mg/L boron), the bar represents the mean ± one standard deviation from two independent experiments. Transformation was calculated as $\left(1-\frac{c_{FIN}}{c_0}\right)\times 100$, where c_0 and c_{FIN} are the initial and final concentrations, respectively. **b** Aliphatic aldehyde concentrations measured after sequential treatment steps; the horizontal red dashed line indicates the target concentration limit in the final effluent of the treatment train. **c** Adsorption behavior of boron on vegetal granular activated carbon (GAC; yellow circles) and granular ferric oxide-hydroxide (GFH; blue squares). **d** Boron concentrations measured across different treatment steps for three independent tests using $NaBH_4$. The horizontal red dashed line again indicates the concentration limit in the final effluent. "n.d." indicates that no data were determined for that specific case.

as an oxidant. However, although NaOCl is more commonly used for its availability and ease of handling, it achieved only partial removal of vanadium, often leaving a substantial residual concentration after the OCF step. Figure 5b additionally shows that, following GAC filtration, vanadium concentrations in the effluent sometimes increased relative to upstream steps. This effect is most likely attributable to the release of trace vanadium impurities present in the GAC material. Because GAC is commonly employed as a polishing step near the end of treatment trains, such release is potentially problematic for meeting effluent quality standards. To address this, a final barrier using GFH was evaluated[53,54]. As shown in Fig. 5a, vanadium was strongly adsorbed onto GFH, as evidenced by the Freundlich isotherm, suggesting effective removal, especially at medium and high concentrations. The vanadium uptake potentially occurs via an anion exchange mechanism involving the formation of binuclear-bridged surface complexes[53]. Panel (b) confirms that GFH filtration consistently reduced vanadium levels to below the regulatory threshold in the final effluent, regardless of GAC-related variability or potential upstream accumulation. This issue of GAC-mediated release was found to extend beyond vanadium: as shown in Fig. S5, similar behavior was observed for aluminum (panel a) and copper (panel b), with GAC effluents showing increased concentrations of these metals in some tests. While measured values did not exceed the respective regulatory targets, the inclusion of GFH as a final filtration step may also offer the multiple benefits of removing aluminum, copper[55], and boron, potentially introduced through the use of sodium borohydride as a reductant (as discussed above), in addition to vanadium.

Performance evaluation of a sequential treatment train

To meet stringent groundwater remediation goals in a matrix containing both conventional pollutants and rarely studied industrial compounds, a lab-scale multibarrier treatment train was designed and experimentally validated at 99.75% water recovery (Fig. 8). Each treatment unit was selected and optimized based on the results of the tests discussed above, as well as practical considerations, such as the formation of problematic compounds (e.g., aliphatic aldehydes), the target of near-zero liquid discharge (99.75% recovery), and ease of full-scale management. Specifically, a high-rejecting seawater RO membrane was used, NaOCl was chosen for OCF, and a multi-stage RO system plus distillation was implemented to achieve near-ZLD. For completeness, post-treatment sections compared chemical reaction routes and two GAC types, ending with GFH filtration to aid in the removal of key residuals like boron and vanadium. The following sections assess performance across all target parameters. For a more detailed and narrative presentation of all the results and discussion, interested readers are encouraged to consult the SI (Supplementary Results S2).

The pre-treatment (OCF + ultrafiltration) targeted suspended solids and oxidizable compounds. Table S4 shows influent values, removals, and effluent concentrations. Results confirmed OCF's effectiveness for methylcyclohexane, naphthalene, and most heavy metals (except vanadium), with >80% removal. In contrast, MDEA, sulfolane, and aliphatic aldehydes showed minimal or negative removal, consistent with preliminary batch tests. Negative removals for MEA, aldehydes, and trihalomethanes point to by-product formation. Vanadium levels increased post-treatment, likely due to oxidative mobilization. Ultrafiltration (UF) removed 82% of TSS but not dissolved contaminants. Fluxes were high (~70-150 kgMH) at 1 ± 0.1 bar, confirming suitability for large-scale solids removal (Fig. 6a). Notably, MEA dropped below detection following UF, suggesting association with particulates formed during OCF.

High-rejection RO membranes (LG Chem SW ES) ensured strong contaminant removal under high-recovery conditions. Figure 6b shows stable fluxes in the first RO stage (9.5 bar), with an expected decline in the second stage (13 bar) and in the third stage (35 bar) as recovery increased. Detailed flux data are reported in Fig. S6, while contaminant removal data are summarized in Table S5 (SI). The results confirmed >99.2% rejection for amines and sulfolane, with final concentrations below detection. Chloride dropped from 324,000 to 2440 µg/L, attesting to the reliability of the test. Aldehyde rejection averaged only 35%, showing the persistence of such compounds. Vanadium rejection was variable (mean 56%, SD 41%), while

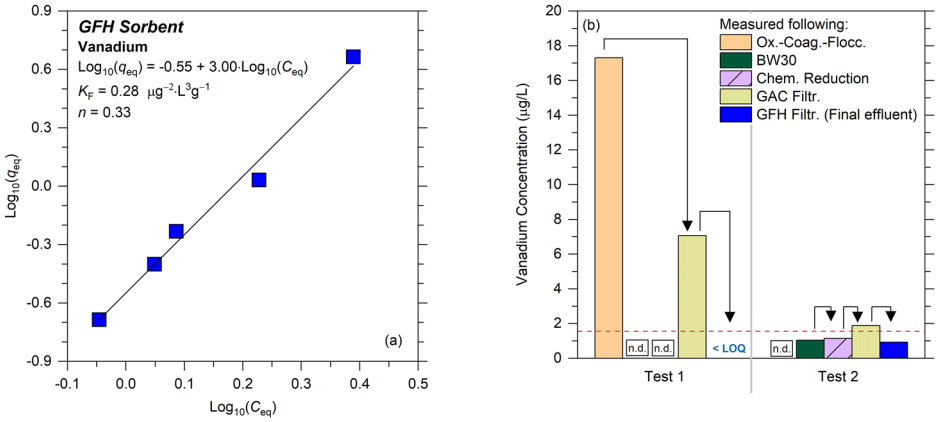

Fig. 5 | Behavior of vanadium during selected treatment steps. a Adsorption isotherm of vanadium onto granular ferric hydroxide (GFH) measured at room temperature. The plot displays experimental data (blue squares) and the corresponding Freundlich model fit (black line), expressed as $q_{eq} = K_F C_{eq}^{\frac{1}{n}}$, and linearized as $Log_{10} q_{eq} = Log_{10} K_F + \frac{1}{n} Log_{10} C_{eq}$. The estimated Freundlich parameters, K_F and n, as well as the linearized equation, are reported in the graph. **b** Vanadium concentrations measured after sequential treatment steps in two independent tests. The red dashed horizontal line indicates the target concentration limit in the final effluent of the treatment train. "n.d." indicates "not determined"; "< LOQ" denotes concentrations below the limit of quantification.

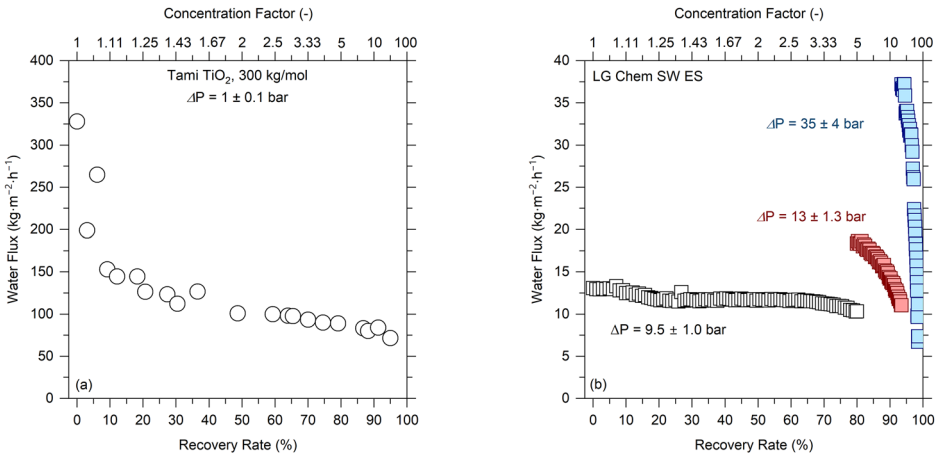

Fig. 6 | Membrane performance in terms of water flux from pilot-scale batch experiments. a Water flux (kgMH) as a function of recovery rate for the ultrafiltration (UF) unit, using a Tami TiO_2 membrane with a molecular weight cutoff of 300 kg/mol. The applied hydraulic pressure difference, ΔP, is indicated in the panel. **b** Water flux (kgMH) as a function of recovery rate for the three stages of reverse osmosis (RO), each using different operating pressures and the same membrane type, as indicated. The top axis reports the corresponding concentration factor, enabling estimation of solute concentration buildup along the treatment process.

boron removal averaged 61%. Distillation of RO concentrate further removed >90% of metals and boron, and efficiently reduced naphthalene. Aldehyde removal (60.4%) was incomplete, further suggesting that subsequent polishing of the effluent is needed. Overall, this treatment section achieved 99.75% recovery and broad contaminant removal, but aldehydes remained problematic.

Post-RO treatments, i.e., $NaBH_4$ reduction, NaOCl oxidation, and O_2 oxidation, were compared (Table S6, SI). $NaBH_4$ effectively removed aldehydes (79.8%) and acetaldehyde (near complete), plus several volatiles and metals, though vanadium remained. Boron slightly increased due to the reducing agent, but remained below 1 mg/L with controlled dosing (3 mg/L). NaOCl removed acetaldehyde, methylcyclohexane, and dichloromethane but failed against aldehydes and generated trihalomethanes. O_2 had low overall effectiveness and formed acetaldehyde. Sulfolane persisted in all cases, though its levels were already compliant.

Final polishing used GAC (vegetal/mineral) and GFH. Table S7 (SI) shows that both GACs removed sulfolane and organohalogens (~100%). Mineral GAC outperformed vegetal GAC for chloroform (94.1% vs. 28.5%) and acetaldehyde (~100% vs. 74.8%). Minor differences were seen for aromatics. Vanadium was released slightly by both GACs (−12.3% mineral, −0.9% vegetal), likely due to impurities. GFH adsorption of vanadium, effective in batch, underperformed here (16.8% mean removal). Several factors may explain this behavior. First, the presence of competing anions, particularly phosphate, silicate, bicarbonate and sulfate, can inhibit vanadium adsorption on iron oxides[56]. In addition, vanadium speciation is pH dependent (e.g., $H_2VO_4^-$ vs. HVO_4^{2-}) and even small variations in pH may influence adsorption affinity[53]. Furthermore, the presence of organic matter and colloids may contribute to fouling or surface site blocking, reducing effective GFH adsorption capacity and kinetics. From a process perspective, shorter contact times and mass-transfer limitation in the continuous system may prevent reaching the equilibrium conditions observed in batch tests. Finally, changes in redox conditions may affect the surface chemistry of the media and vanadium binding mechanisms. Unexpected tribromomethane formation (−105% removal) was noted in GFH filtration, but levels stayed below limits.

Synthesis and final evaluation of the sequential treatment train

The concentration of eight representative compounds across the system train is plotted in Fig. 7: sulfolane, amines, aliphatic aldehydes, organohalogens, naphthalene, heavy metals (excluding vanadium), vanadium, and boron. Data in Fig. 7 refer to trains with vegetal GAC. Sulfolane was partly removed by OCF, then fully by RO and distillation. Amines spiked post-OCF but became undetectable after RO. Aldehydes rose after OCF and resisted RO/distillation; $NaBH_4$ reduced them effectively, unlike NaOCl or O_2. GAC/GFH offered limited further polishing of aldehydes.

Organohalogens increased after OCF but were removed effectively thereafter. Naphthalene was reduced by OCF/UF but persisted post-GAC, suggesting a second GAC step may be needed at full scale. Heavy metals stayed below limits except for occasional post-GFH increases (e.g., Mn, Cu), implying better robustness of the train without GFH. Vanadium behavior was erratic, and GFH failed to remove it. Boron was stable or reduced, with expected increase from $NaBH_4$, yet always below limits, and further reduced by GAC + GFH. It is worth noting that the release of trace metals from GAC and GFH observed in this study is likely due to intrinsic media impurities

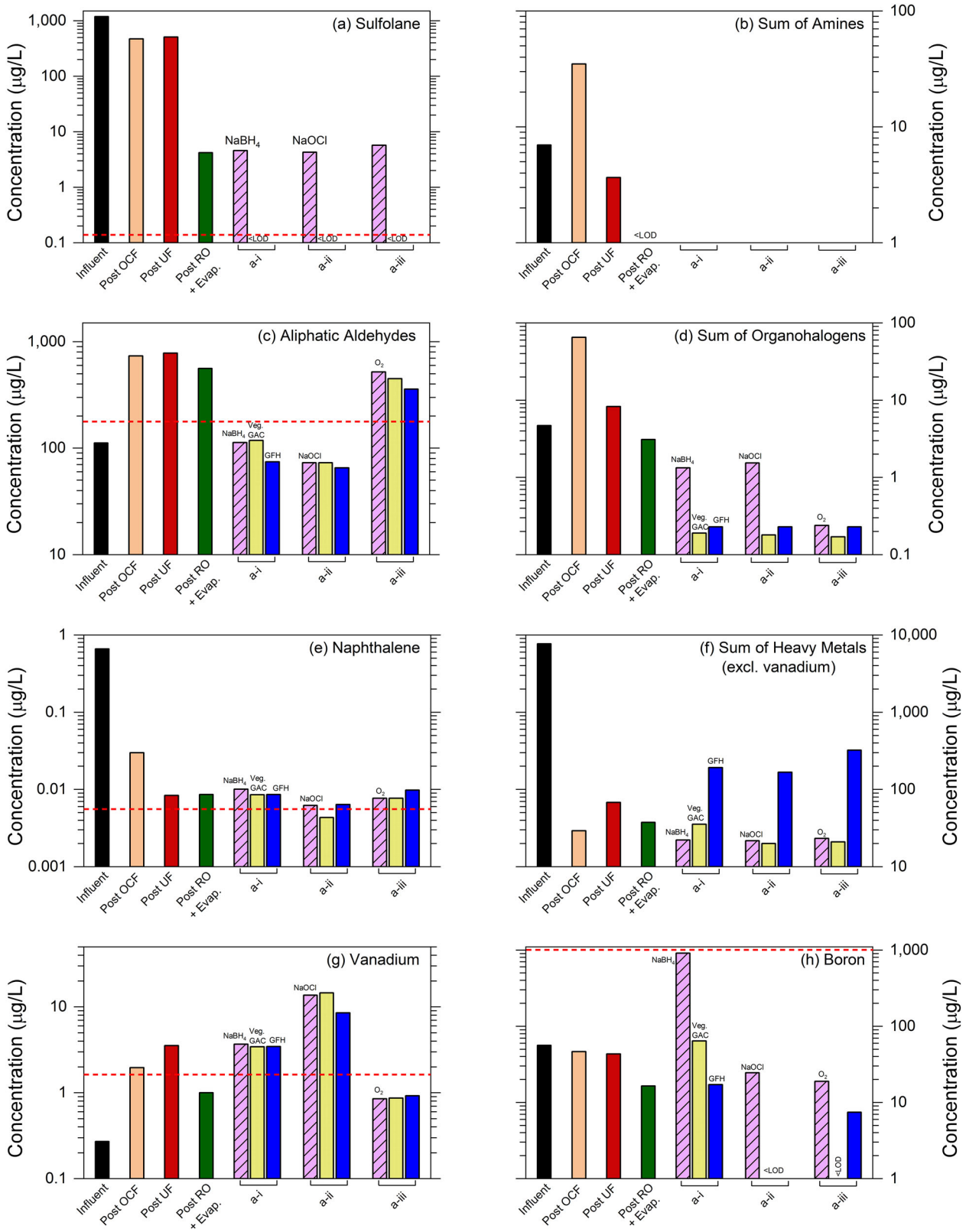

Fig. 7 | Concentrations of selected compounds or compound classes measured after sequential treatment steps. The red dashed horizontal line indicates the target concentration limit in the final effluent of the treatment train. "< LOD" denotes concentrations below the limit of detection. Bar colors correspond to the following sampling points: Black: influent; Light orange: effluent of oxidation–coagulation–flocculation (OCF); Red: effluent of ultrafiltration (UF); Green: combined permeate from the three reverse osmosis (RO) stages and distillate from the distiller; Patterned violet: effluent of the chemical reaction step; Dotted yellow: effluent of granular activated carbon (GAC) filtration; Blue: effluent of granular ferric oxide-hydroxide (GFH) filtration. Values are shown for three treatment trains differing in the chemical reaction step, all followed by vegetal GAC filtration: (**a-i**) reduction with sodium borohydride, (**a-ii**) oxidation with sodium hypochlorite, (**a-iii**) oxidation with molecular oxygen.

and desorption under changing water chemistry (e.g., variations in ionic strength, pH, or concentration factor). This effect was particularly evident when fresh media was first contacted and under high concentration conditions. While these phenomena may affect initial effluent quality, they can be mitigated in full-scale applications through standard media preconditioning procedures, including rinsing, pre-washing, and bed flushing until stable effluent quality is achieved. Optimization of these procedures is recommended for full-scale operation, although a detailed investigation was beyond the scope of this study.

The accordance between the results obtained in preliminary tests and in the sequential treatment supports the robustness of the experimental methods and observations. The complete treatment train performance data are reported in Figs. S7, S8, and S9 (SI), in which contaminants showing critical effluent concentrations are highlighted in orange. In summary, the conceptualized and tested multi-barrier train, centered on high-rejection RO with optimized pre-/post-treatments, effectively removed most contaminants under near-ZLD conditions. Yet, aldehydes, naphthalene, vanadium, and some metals remained challenging. The underperformance of GFH and occasional metal release from this material suggest that replacing it with a second GAC filter may enhance robustness and polishing effectiveness of the treatment train at full scale.

A preliminary economic assessment of the proposed system is presented based on calculations and input from specialized engineering companies. The estimated capital expenditure (CAPEX) for the construction of a treatment plant of this scale, designed to handle an average flow rate of 36 m^3/h and peak flows of 130 m^3/h, ranges between €15 and €17 million. The annual operational expenditure (OPEX), including labor, maintenance, chemical reagents, and waste management and disposal, is estimated at €2.5–3.5 million. In comparison to the current treatment strategy (pumping out with off-site disposal), the proposed system is expected to reduce operational costs by approximately 40–45%. This reduction is mainly driven by the substantial decrease in waste volume requiring disposal (~99.75%). Given a disposal cost ranging between 130 and 170 €/m^3, this reduction represents a major economic advantage. The discounted payback period (DPP) was estimated with the following equation[57]:

$$DPP = \textit{the first year } t \textit{ such that } : \sum_{i=1}^{t} \frac{\textit{Net yearly savings}}{(1+r)^i} \geq CAPEX \quad (1)$$

where the net yearly savings correspond to reduction in OPEX and r is the discount rate. Assuming a CAPEX of €15–17 million, a net yearly saving of conservatively €2 million, and a discount rate of 7%, the DPP is estimated to be between 9.5 and 10.5 years. Therefore, considering a system lifetime of 15 years, the proposed solution is economically viable and yields a positive return within its operational horizon.

Overall, the proposed configuration offers relevant environmental and economic advantages. The high-quality effluent enables safe discharge to surface water bodies, while the extremely limited concentrate volume significantly reduces handling and disposal requirements. When coupled with the positive economic return indicated by the preliminary assessment, these results support the practical viability of near-ZLD approaches for contaminated groundwater treatment. More broadly, this work suggests that the implementation of high-recovery treatment concepts is not only technically achievable but also economically justified, and could be extended to a wide range of pump-and-treat systems for fresh to mildly mineralized contaminated groundwater.

Methods

Feed water characteristics and effluent limits

All experiments were conducted on untreated groundwater extracted from an active industrial remediation site, thus preserving the complexity of competing solutes and transformation products. Specifically, the groundwater was sourced from a contaminated site in Italy, located in a hydrocarbon processing area, and was characterized by a complex mixture of organic and inorganic pollutants. The investigated water matrix is highly representative of shallow aquifers in anthropogenically impacted or industrial areas. While hydrochemistry may vary, fresh to mildly mineralized aquifers (TDS typically <1000 mg/L) represent the largest fraction of contaminated industrial sites globally[58,59]. Table 1 summarizes influent average and peak concentrations of contaminants exceeding regulatory limits, alongside target effluent levels and corresponding removal requirements for discharge onto surface water bodies. The characteristics of the water used for the laboratory experiment were consistent with the average expected concentration reported below. A more comprehensive overview, including the full list of contaminants and the rationale for effluent limits, is provided in Figure S1 (SI). Effluent concentration limits were primarily based on Italian national legislation for discharge into surface waters (D.Lgs 152/2006). For non-regulated parameters, effluent limits coincided with the instrumental limits of detection (LOD), as they provide a conservative and enforceable criterion in the absence of regulatory thresholds. Alternatively, stringent performance targets were agreed upon with the competent environmental authorities, as in the case of aldehydes. The LOD values are provided in Table S1 (SI).

The groundwater was sourced from a fresh to mildly mineralized aquifer showing, for average and peak influent concentration conditions, respectively, total dissolved solids (TDS) equal to 400 mg/L and 600 mg/L, chemical oxygen demand (COD) equal to 11 mg/L and 105 mg/L, and total suspended solids (TSS) equal to 5 mg/L and 15 mg/L. Target contaminants included: metals, most notably iron, aluminum, zinc, and manganese, as well as boron; volatile organics and solvents, such as dichloromethane, methyl isobutyl ketone (MIBK), and methyl ethyl ketone (MEK); and organic compounds like sulfolane and several alkanolamines, namely, (mono)ethanolamine (MEA), diethanolamine (DEA), methyldiethanolamine (MDEA), and triethanolamine (TEA), which are poorly biodegradable and require advanced treatment technologies[25,60,61]. These compounds required high removal efficiencies, due to strict discharge thresholds (e.g., sulfolane, detected at concentrations up to the mg/L range, had to be reduced to below 1 µg/L, necessitating >99.96% removal). The treatment system was therefore designed to ensure robust, multibarrier contaminant removal, a high water recovery rate (99.75%), and minimal production of residual waste and sludge.

Materials and water analyses

All reagents used in this study were of at least reagent grade (≥99.9% purity). Unless otherwise specified, all reagents were purchased from Carlo Erba (Milan, Italy), except for NaOCl, which was sourced from Thermo Fisher Scientific (Monza, Italy). Where required, deionized water was obtained with a Milli-Q system (Milli-Q® IX 7005, 323 Merck Millipore, Darmstadt, Germany). All analytical determinations were conducted by an external accredited laboratory, LabAnalysis (Casanova Lonati, Pavia, Italy), certified to UNI CEI EN ISO/IEC 17025:2018 standards. The full list of analytical methods is reported in Table S2 of the SI.

Preliminary experiments

A series of preliminary experiments was conducted to evaluate the effectiveness of various unit operations in removing target contaminants. Chemical pre-treatment of the contaminated groundwater was performed using a pre-oxidation–coagulation–flocculation (OCF) process designed to promote the removal of metals, suspended solids, and the oxidative transformation of electron-rich organic compounds[36,41]. Reagents were applied to achieve final concentrations of 22 mg/L of NaOCl or ClO_2, 58 mg/L of $FeCl_3$ (equivalent to 20 mgFe/L), 40 mg/L of NaOH, 4 mg/L of polyelectrolyte, and 20 mg/L of HCl. Briefly, the oxidant (NaOCl or ClO_2) was dosed into the groundwater sample and stirred (~700 rpm) for 1 min, before simultaneous addition of $FeCl_3$ and NaOH. pH was adjusted to 10 while maintaining the same stirring conditions for an additional 3 min. The polyelectrolyte was then added, and slow mixing (20 min, ~50 rpm) allowed floc formation and stabilization. pH was then adjusted to 9.0 ± 0.5, in accordance with effluent discharge limits (Italian regulation D.Lgs. 152/06) and left to settle for

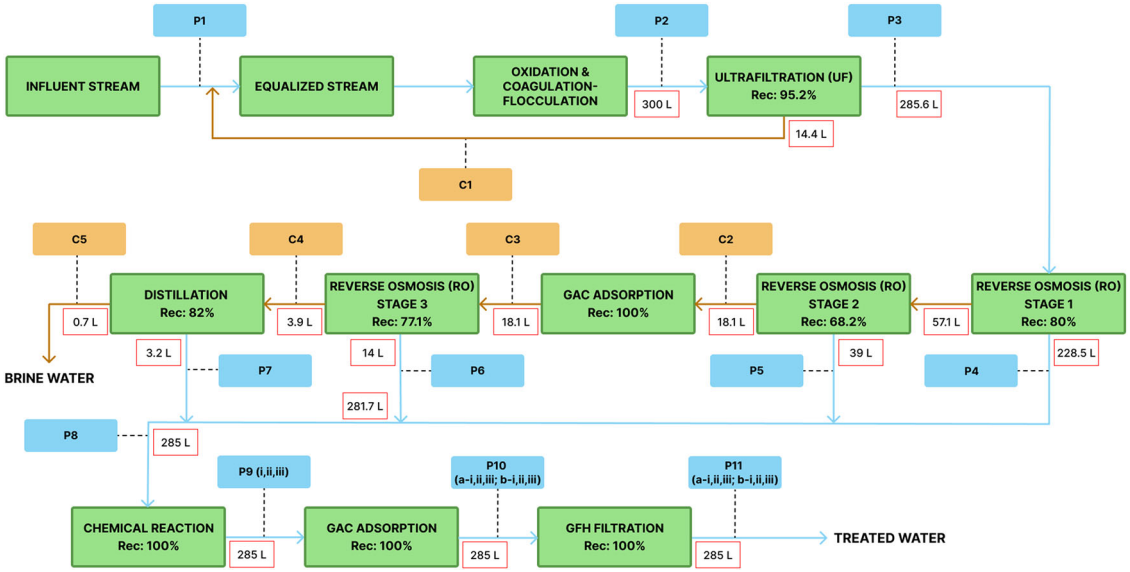

Fig. 8 | Block diagram of the treatment train developed for the remediation of contaminated groundwater. Green boxes indicate the unit processes investigated in this study. Blue arrows represent treated effluent streams, while orange arrows correspond to concentrate streams generated by unit operations with recovery rates below 100%. Recovery rate values are reported within the green boxes. The overall treatment train achieved a total water recovery of 99.75%. Volumes of water utilized in the experimentation are shown in small white boxes with red outlines. Sampling points are marked with blue or orange boxes, where "P" denotes permeate streams and "C" denotes concentrate streams. Three chemical oxidation/reduction processes were tested (i: reduction with sodium borohydride; ii: oxidation with sodium hypochlorite; iii: oxidation with molecular oxygen), as well as two granular activated carbon (GAC) materials in the polishing step (a: vegetal GAC; b: mineral GAC).

30 min before separation of the clarified supernatant. Each test with NaOCl or ClO_2 was conducted in triplicate.

Granular activated carbon (GAC) adsorption was evaluated as a core treatment process for removing recalcitrant organic compounds, with its performance for sulfolane and alkanolamines adsorption (MEA, DEA, MDEA, TEA) still underexplored[62–64]. GAC adsorption is mainly governed by hydrophobic interactions and π–π interactions. Consequently, adsorption affinity generally increases with molecular size and decreases with polarity, leading to an efficient removal of large organic (hydrophobic) compounds, and a limited removal of small, hydrophilic compounds[63]. Batch adsorption tests were conducted on OCF-treated groundwater, either as received or after spiking with contaminants while preserving their original mass concentration ratios. In all cases, GAC (0–50 g/L) was dosed into 200 mL of sample in sealed glass vessels. After 24 h of magnetic stirring at room temperature, supernatants were filtered and analyzed for residual concentrations. Adsorption isotherms were fitted using the Freundlich model. Steam-activated, virgin GAC (SC 1240), compliant with UNI EN 12915-1 for drinking water, was used. To complement batch data, 8-week-long column tests were conducted using two parallel plexiglass columns (diameter 1.6 cm and ~35 cm GAC bed depth), fed with OCF-treated water. The flow rate was ~2 mL/min (empty bed contact time, EBCT, ~30 min). The effluent was sampled periodically, and breakthrough trends were analyzed.

Lab-scale reverse osmosis (RO) experiments evaluated the performance of polyamide thin-film composite membranes (DuPont FilmTec™ XLE, BW30, and SW30). Commercial flat-sheet coupons were tested in a closed-loop cross-flow set-up under manufacturer-recommended pressures. The feed tank was kept at 13 ± 1 °C. Permeate water was collected until ~75% water recovery was achieved, and permeate flux was manually measured at every 10% increment in recovery. Compound "system rejection" was used to assess membrane performance. To support the integration of RO with polishing steps, complementary experiments were also run combining OCF, RO (DuPont BW30, 65–80% recovery), and permeate post-treatments: (i) chemical reduction with $NaBH_4$ (2 mg/L, 24 h), and (ii) sequential filtration through GAC and granular ferric oxide-hydroxides (GFH; see below for further information on this material) in series (column test conditions: 1.6 cm ID, 35 cm bed, EBCT ~ 30 min, flow 2 mL/min).

Chemical reduction with sodium borohydride ($NaBH_4$) targeted the transformation of aliphatic aldehydes into more readily adsorbable species[48,65]. A first test (100 mg/L $NaBH_4$) demonstrated proof-of-concept, followed by lower-dose tests (2 and 5 mg/L) to assess feasibility and residual boron compliance (≤1 mg/L per D.Lgs. 152/2006). For each test, 10 L of OCF-treated groundwater was used, with reactions conducted in sealed vessels under continuous stirring at room temperature for 24 h. The treated water was subjected to batch adsorption on GAC, or column filtration (GAC, or GAC followed by GFH), to assess removal efficiency under possible potential overdosing scenarios.

GFH (β-FeOOH and $Fe(OH)_3$) was tested as a polishing step post-GAC targeting residual metals, particularly vanadium and copper. Batch tests used GAC effluent with GFH doses of 1–30 g/L, stirred for 24 h. Plexiglass columns were used for column tests (diameter 1.6 cm and ~35 cm GAC bed depth), with water pumped at 2 mL/min (EBCT ~ 30 min).

Design and evaluation of the full treatment train

The integrated, sequential treatment train was designed to achieve high removal rates across a broad spectrum of organic and inorganic contaminants while minimizing residual waste and maximizing water recovery (target: 99.75%). The system layout, stream volumes, and sampling points are summarized in Fig. 8. The influent water was first subjected to (a) pre-treatment via an OCF process and UF to remove suspended solids and oxidizable species. This step was followed by (b) concentration, achieved through RO across three stages and distillation of the final concentrate. The mix of permeates and distillate was then subjected to a series of post-treatment steps, including (c) chemical reaction, as well as (d) polishing by filtration through GAC and ferric oxide-hydroxide adsorption (GFH).

In the pre-treatment section, OCF was performed as outlined above with NaOCl as pre-oxidant. Following coagulation and flocculation, 300 L of supernatant was treated with a ceramic UF membrane (TAMI, TiO2, 300 kg/mol, 0.21 m^2 active area) operating in cross-flow mode at 1 ± 0.1 bar. System recovery was 95.2%, yielding 285.6 L permeate and 14.4 L concentrate (fully recirculated to OCF in the full system design).

To achieve concentration, the UF permeate was first treated through a staged RO system. The first stage processed 285.6 L of water at 9.5 ± 1.0 bar using LG Chem SW ES membranes, and achieved 80.0% recovery (228.5 L

of permeate and 57.1 L of concentrate). The concentrate was then fed to the second RO stage, operated at 13 ± 1.3 bar, with a recovery of 68.2%. This stage generated 39.0 L of permeate and 18.1 L of concentrate. The latter was further treated with GAC (vegetal origin, SC 1240) in a packed-bed column to reduce organic load prior to the third RO stage. The third stage operated at 35 ± 4 bar and produced 14 L of permeate and 4.1 L of concentrate (77.1% recovery). The final RO concentrate was processed via thermal distillation at 90 °C, under mild vacuum conditions, achieving 82% water recovery 3.4 L of distillate and 0.7 L of residual brine. The distillate was combined with the three RO permeates to obtain a treated water mixture totaling 285 L (i.e., 80.23% RO stage 1 permeate, 13.68% RO stage 2, 4.92% RO stage 3, 1.17% distillate), which was used as the feed for the post-treatment sections.

Three chemical reaction pathways were tested in parallel: (i) chemical reduction with sodium borohydride (3 mg/L), (ii) oxidation with sodium hypochlorite (7.5 mg/L), and (iii) oxidation with dissolved oxygen to saturation. Each reaction was conducted in batch mode for 15 min at ambient temperature and under gentle stirring. For the sodium borohydride reduction, the reaction was carried out at pH 10.3. After 15 min, the solution was acidified using hydrochloric acid (HCl, 1 M) to arrest the reduction process and bring the pH within the target effluent range of 5.5–9.5. For the sodium hypochlorite oxidation, the reaction was maintained at pH 7.7 with an ORP of approximately 600 mV. Following the reaction, quenching was performed using sodium metabisulfite (Na2S2O5) (Note that bisulfite ions can form reversible adducts with aldehydes. Consequently, when present in excess, bisulfite formed upon the addition of $Na_2S_2O_5$ can significantly reduce the detectable concentration of free aldehydes. This effect may interfere with aldehyde determination, particularly in spectrophotometric or titrimetric methods, such as that used in this study (APAT CNR IRSA 5010 A Man 29, 2003), that rely on the quantification of unbound aldehydes. For the oxidation with dissolved oxygen, excess oxygen was bubbled into the solution for 15 min to reach saturation. The reaction occurred at pH 8.8 with an ORP of approximately 340 mV, which decreased to 315 mV shortly after aeration was stopped. No quenching was required in this case, and the pH remained within acceptable limits.

In the polishing section, the chemically treated water was then passed through GAC columns packed with either (a) the same SC 1240 (vegetal-based) GAC used for preliminary tests or (b) Organosorb 10 (mineral-based) GAC. Organosorb 10 has a particle size distribution of 0.60–2.36 mm, with at least 90% of particles under 2.36 mm and 93% over 0.60 mm (ASTM D2862). Its bulk density is approximately 500 kg/m^3, with a BET-specific surface area of 960 m^2/g and a minimum iodine number of 950 mg/g. Both GAC types were pre-rinsed and hydrated prior to use. The columns had a bed height of 35 cm, an internal diameter of 1.6 cm, and were operated at an empty bed contact time of 15 min. The flow rate was maintained at approximately 4.7 mL/min using peristaltic pumps. Effluent from each GAC column was directed into a second packed column containing GFH. The GFH columns operated under identical hydraulic conditions as the GAC columns. For each combination of chemical treatment and GAC type, a full treatment path was tested. Samples were collected at the outlet of each unit and analyzed for all target parameters to assess treatment performance.

Data availability

Data generated or analyzed during this work are included in this manuscript and its supplementary information file. Raw data can be made available from the authors upon request.

Received: 18 February 2026; Accepted: 6 April 2026;
Published online: 11 June 2026

References

1. Li, P., Karunanidhi, D., Subramani, T. & Srinivasamoorthy, K. Sources and consequences of groundwater contamination. *Arch. Environ. Contam. Toxicol.* **80**, 1–10 (2021).
2. Pradhan, B., Chand, S., Chand, S., Rout, P. R. & Naik, S. K. Emerging groundwater contaminants: a comprehensive review on their health hazards and remediation technologies. *Groundw. Sustain. Dev.* **20**, 100868 (2023).
3. Karandish, F., Liu, S., & de Graaf, I. Global groundwater sustainability: a critical review of strategies and future pathways. *J. Hydrol*. **657**, 133060 (2025).
4. UNESCO World Water Assessment Programme. *The United Nations World Water Development Report 2018: Nature-based Solutions for Water*. Available: https://unesdoc.unesco.org/ark:/48223/pf0000261424.
5. Reberski, J. L., Terzić, J., Maurice, L. D. & Lapworth, D. J. Emerging organic contaminants in karst groundwater: a global level assessment. *J. Hydrol.* **604**, 127242 (2022).
6. Bunting, S. et al. Emerging organic compounds in European groundwater. *Environ. Pollut.* **269**, 115945 (2021).
7. Preisner, M., Neverova-Dziopak, E. & Kowalewski, Z. An analytical review of different approaches to wastewater discharge standards with particular emphasis on nutrients. *Environ. Manag.* **66**, 694–708 (2020).
8. European Environment Agency. *European Waters: Assessment of Status and Pressures 2018*. Report No 7/2018. Available: https://www.eea.europa.eu/publications/state-of-water.
9. Ho, J. et al. Assuring reclaimed water quality using a multi-barrier treatment train according to the new EU non-potable water reuse regulation. *Water Res.* **267**, 122429 (2024).
10. Ahmed, S. et al. Recent developments in physical, biological, chemical, and hybrid treatment techniques for removing emerging contaminants from wastewater. *J. Hazard. Mater.* **416**, 125912 (2021).
11. Schwarzenbach, R. P. et al. The challenge of micropollutants in aquatic systems. *Science* **313**, 1072–1077 (2006).
12. Veselská, V. et al. Unveiling trends in migration of iron-based nanoparticles in saturated porous media. *J. Environ. Manag.* **370**, 122552 (2024).
13. Latif, A. et al. Remediation of heavy metals polluted environment using Fe-based nanoparticles: Mechanisms, influencing factors, and environmental implications. *Environ. Pollut.* **264**, 114728 (2020).
14. Obiri-Nyarko, F., Grajales-Mesa, S. J. & Malina, G. An overview of permeable reactive barriers for in situ sustainable groundwater remediation. *Chemosphere* **111**, 243–259 (2014).
15. Mystrioti, C. & Papassiopi, N. A comprehensive review of remediation strategies for soil and groundwater contaminated with explosives. *Sustainability* **16**, 961 (2024).
16. Higgins, M. R. & Olson, T. M. Life-cycle case study comparison of permeable reactive barrier versus pump-and-treat remediation. *Environ. Sci. Technol.* **43**, 9432–9438 (2009).
17. Sethi, R. & Molfetta, A., *Groundwater engineering*. Springer, 2019.
18. Shahid, M. K., Kashif, A., Fuwad, A. & Choi, Y. Current advances in treatment technologies for removal of emerging contaminants from water–A critical review. *Coord. Chem. Rev.* **442**, 213993 (2021).
19. Lima, E. C. Removal of emerging contaminants from the environment by adsorption. *Ecotoxicol. Environ. Saf.* **150**, 1–17 (2018).
20. Sheng, C., Nnanna, A. A., Liu, Y. & Vargo, J. D. Removal of Trace Pharmaceuticals from Water using coagulation and powdered activated carbon as pretreatment to ultrafiltration membrane system. *Sci. Total Environ.* **550**, 1075–1083 (2016).
21. Rizzo, L. et al. Consolidated vs new advanced treatment methods for the removal of contaminants of emerging concern from urban wastewater. *Sci. Total Environ.* **655**, 986–1008 (2019).
22. Tong, T. & Elimelech, M. The global rise of zero liquid discharge for wastewater management: drivers, technologies, and future directions. *Environ. Sci. Technol.* **50**, 6846–6855 (2016).

23. Yaqub, M. & Lee, W. Zero-liquid discharge (ZLD) technology for resource recovery from wastewater: A review. *Sci. Total Environ.* **681**, 551–563 (2019).
24. Abdelfattah, I. & El-Shamy, A. Review on the escalating imperative of zero liquid discharge (ZLD) technology for sustainable water management and environmental resilience. *J. Environ. Manag.* **351**, 119614 (2024).
25. Dinh, M., Hakimabadi, S. G. & Pham, A. L.-T. Treatment of sulfolane in groundwater: a critical review. *J. Environ. Manag.* **263**, 110385 (2020).
26. Pensini, E., Hsiung, C. & Kashlan, N. Potential toxic effects linked to taurine interactions with alkanolamines and diisopropylamine. *Discov. Water* **4**, 86 (2024).
27. Rehnstam, S., Smith, S. J. & Ahrens, L. Suspect and non-target screening of per-and polyfluoroalkyl substances (PFAS) and other halogenated substances in electrochemically oxidized landfill leachate and groundwater. *J. Hazard. Mater.* **480**, 136316 (2024).
28. Yu, L., Khan, M. F. & Achari, G. A review on physiochemical treatment of sulfolane in aqueous media. *J. Environ. Chem. Eng.* **9**, 105691 (2021).
29. Dong, C. et al. Wastewater treatment in amine-based carbon capture. *Chemosphere* **222**, 742–756 (2019).
30. Shah, A. D. & Mitch, W. A. Halonitroalkanes, halonitriles, haloamides, and N-nitrosamines: a critical review of nitrogenous disinfection byproduct formation pathways. *Environ. Sci. Technol.* **46**, 119–131 (2012).
31. Marron, E. L. et al. Reactions of α, β-unsaturated carbonyls with free chlorine, free bromine, and combined chlorine. *Environ. Sci. Technol.* **55**, 3305–3312 (2021).
32. Guo, K., Wu, Z., Chen, C. & Fang, J. UV/chlorine process: an efficient advanced oxidation process with multiple radicals and functions in water treatment. *Acc. Chem. Res.* **55**, 286–297 (2022).
33. Mitch, W. A. & Schreiber, I. M. Degradation of tertiary alkylamines during chlorination/chloramination: implications for formation of aldehydes, nitriles, halonitroalkanes, and nitrosamines. *Environ. Sci. Technol.* **42**, 4811–4817 (2008).
34. Tian, C., Liu, R., Liu, H. & Qu, J. Disinfection by-products formation and precursors transformation during chlorination and chloramination of highly-polluted source water: significance of ammonia. *Water Res.* **47**, 5901–5910 (2013).
35. Fan, X. & Sokorai, K. J. Formation of trichloromethane in chlorinated water and fresh-cut produce and as a result of reaction with citric acid. *Postharvest Biol. Technol.* **109**, 65–72 (2015).
36. Wang, Z. et al. Formation of halogenated by-products during chemical cleaning of humic acid-fouled UF membrane by sodium hypochlorite solution. *Chem. Eng. J.* **332**, 76–84 (2018).
37. Sangamnere, R., Misra, T., Bherwani, H., Kapley, A. & Kumar, R. A critical review of conventional and emerging wastewater treatment technologies. *Sustain. Water Resour. Manag.* **9**, 58 (2023).
38. Marron, E. L., Mitch, W. A., von Gunten, U. & Sedlak, D. L. A tale of two treatments: the multiple barrier approach to removing chemical contaminants during potable water reuse. *Acc. Chem. Res.* **52**, 615–622 (2019).
39. Kienle, C. et al. Evaluation of a full-scale wastewater treatment plant with ozonation and different post-treatments using a broad range of in vitro and in vivo bioassays. *Water Res.* **212**, 118084 (2022).
40. Al-Hamzah, A. A. et al. Use of chlorine dioxide as alternative to chlorination in reverse osmosis product water. *Desalin. Water Treat.* **163**, 57–66 (2019).
41. Gordon, G. & Rosenblatt, A. A. Chlorine dioxide: the current state of the art. *Ozone Sci. Eng.* **27**, 203–207 (2005).
42. Yang, X., Guo, W. & Lee, W. Formation of disinfection byproducts upon chlorine dioxide preoxidation followed by chlorination or chloramination of natural organic matter. *Chemosphere* **91**, 1477–1485 (2013).
43. Black & Veatch Corporation. *White's Handbook of Chlorination and Alternative Disinfectants* (John Wiley & Sons, 2011).
44. Neguez, S. & Laky, D. Byproduct formation of chlorination and chlorine dioxide oxidation in drinking water treatment: their formation mechanisms and health effects. *Period. Polytech. Chem. Eng.* **67**, 367–385 (2023).
45. Kunigk, L., Gedraite, R., & Jurkiewicz Kunigk, C. Efficacy of chlorine dioxide and sodium hypochlorite in reuse water disinfection. *Environ. Eng. Manag. J.* **17**, https://doi.org/10.30638/EEMJ.2018.072 (2018).
46. Palma, P. et al. Membranes technology used in water treatment: chemical, microbiological and ecotoxicological analysis. *Sci. Total Environ.* **568**, 998–1009 (2016).
47. Marron, E. L., Prasse, C., Buren, J. V. & Sedlak, D. L. Formation and fate of carbonyls in potable water reuse systems. *Environ. Sci. Technol.* **54**, 10895–10903 (2020).
48. Li, X. et al. Unravelling the underlying mechanism of the reduction of aldehydes/ketones with metal borohydride in an aprotic solvent. *Chem. Commun.* **60**, 5486–5489 (2024).
49. Anderson, A. et al. Treatment of heavy metals containing wastewater using biodegradable adsorbents: a review of mechanism and future trends. *Chemosphere* **295**, 133724 (2022).
50. Deng, Y. & Zhao, R. Advanced oxidation processes (AOPs) in wastewater treatment. *Curr. Pollut. Rep.* **1**, 167–176 (2015).
51. Lin, J.-Y., Mahasti, N. N. & Huang, Y.-H. Recent advances in adsorption and coagulation for boron removal from wastewater: a comprehensive review. *J. Hazard. Mater.* **407**, 124401 (2021).
52. Guan, Z., Lv, J., Bai, P. & Guo, X. Boron removal from aqueous solutions by adsorption—A review. *Desalination* **383**, 29–37 (2016).
53. Naeem, A., Westerhoff, P. & Mustafa, S. Vanadium removal by metal (hydr) oxide adsorbents. *Water Res.* **41**, 1596–1602 (2007).
54. Dabizha, A., Bahr, C. & Kersten, M. Predicting breakthrough of vanadium in fixed-bed absorbent columns with complex groundwater chemistries: a multi-component granular ferric hydroxide– vanadate – arsenate– phosphate– silicic acid system. *Water Res. X* **9**, 100061 (2020).
55. Steiner, M., Pronk, W. & Boller, M. A. Modeling of copper sorption onto GFH and design of full-scale GFH adsorbers. *Environ. Sci. Technol.* **40**, 1629–1635 (2006).
56. Youngran, J., Maohong, F., Van Leeuwen, J. & Belczyk, J. F. Effect of competing solutes on arsenic (V) adsorption using iron and aluminum oxides. *J. Environ. Sci.* **19**, 910–919 (2007).
57. White, J. A., Grasman, K. S., Case, K. E., Needy, K. L., & Pratt, D. B. *Fundamentals of Engineering Economic Analysis* (John Wiley & Sons, 2020).
58. Selvakumar, S., Chandrasekar, N. & Kumar, G. Hydrogeochemical characteristics and groundwater contamination in the rapid urban development areas of Coimbatore, India. *Water Resour. Ind.* **17**, 26–33 (2017).
59. Xiao, J. et al. Groundwater hydrochemistry, source identification and pollution assessment in intensive industrial areas, eastern Chinese loess plateau. *Environ. Pollut.* **278**, 116930 (2021).
60. Buvik, V., Vevelstad, S. J., Brakstad, O. G. & Knuutila, H. K. Stability of structurally varied aqueous amines for CO2 capture. *Ind. Eng. Chem. Res.* **60**, 5627–5638 (2021).
61. Harimurti, S., Omar, A. A., Rahmah, A. U., & Murugesan, T. The degradation mechanism of wastewater containing MDEA using UV/H 2 O 2 advanced oxidation process. in *Proc. 2011 National Postgraduate Conference*, 1–5 (IEEE, 2011).
62. Yankovych, H., Melnyk, I. & Václavíková, M. Understanding of mechanisms of organohalogens removal onto mesoporous granular activated carbon with acid-base properties. *Micropor. Mesopor. Mat.* **317**, 110974 (2021).

63. Eeshwarasinghe, D., Loganathan, P. & Vigneswaran, S. Simultaneous removal of polycyclic aromatic hydrocarbons and heavy metals from water using granular activated carbon. *Chemosphere* **223**, 616–627 (2019).
64. Valderrama, C., Gamisans, X., De las Heras, X., Farran, A. & Cortina, J. Sorption kinetics of polycyclic aromatic hydrocarbons removal using granular activated carbon: intraparticle diffusion coefficients. *J. Hazard. Mater.* **157**, 386–396 (2008).
65. Johnson, M. R. & Rickborn, B. Sodium borohydride reduction of conjugated aldehydes and ketones. *J. Org. Chem.* **35**, 1041–1045 (1970).

Acknowledgements

The experimental activity was performed in the interdepartmental Clean Water Center (CWC). This work was partly funded by Eni Rewind S.p.A.

Author contributions

L.C. and E.B. contributed to conceptualization, methodology development, investigation, data curation, formal analysis, visualization, and writing of the manuscript through review and editing. M.M., G.C., and D.C. contributed to investigation, methodology, data curation, formal analysis, visualization, and manuscript review and editing. A.Tr. and V.R. contributed resources and participated in manuscript review and editing. A.Ti. contributed to methodology, formal analysis, data curation, visualization, validation, and supervision, drafted the original manuscript, and was responsible for resources, project administration, and funding acquisition. All authors read and approved the final manuscript.

Competing interests

The authors declare no competing interests.

Additional information

Supplementary information The online version contains supplementary material available at https://doi.org/10.1038/s41545-026-00579-2.

Correspondence and requests for materials should be addressed to Alberto Tiraferri.

Reprints and permissions information is available at http://www.nature.com/reprints

Publisher's note Springer Nature remains neutral with regard to jurisdictional claims in published maps and institutional affiliations.

Open Access This article is licensed under a Creative Commons Attribution 4.0 International License, which permits use, sharing, adaptation, distribution and reproduction in any medium or format, as long as you give appropriate credit to the original author(s) and the source, provide a link to the Creative Commons licence, and indicate if changes were made. The images or other third party material in this article are included in the article's Creative Commons licence, unless indicated otherwise in a credit line to the material. If material is not included in the article's Creative Commons licence and your intended use is not permitted by statutory regulation or exceeds the permitted use, you will need to obtain permission directly from the copyright holder. To view a copy of this licence, visit http://creativecommons.org/licenses/by/4.0/.

© The Author(s) 2026